Clim Dyn
DOI 10.1007/s00382-015-2800-1

The 2014 southeast Brazil austral summer drought: regional scale mechanisms and teleconnections

Caio A. S. Coelho[1] · Cristiano Prestrelo de Oliveira[2] · Tércio Ambrizzi[2] · Michelle Simões Reboita[3] · Camila Bertoletti Carpenedo[2] · José Leandro Pereira Silveira Campos[2] · Ana Carolina Nóbile Tomaziello[2] · Luana Albertani Pampuch[2] · Maria de Souza Custódio[2] · Lívia Marcia Mosso Dutra[2] · Rosmeri P. Da Rocha[2] · Amanda Rehbein[2]

Received: 5 February 2015 / Accepted: 8 August 2015
© Springer-Verlag Berlin Heidelberg 2015

Abstract The southeast region of Brazil experienced in austral summer 2014 a major drought event leading to a number of impacts in water availability for human consumption, agricultural irrigation and hydropower production. This study aims to perform a diagnostic analysis of the observed climate conditions during this event, including an inspection of the occurred precipitation anomalies in the context of previous years, and an investigation of possible relationships with sea surface temperatures and atmospheric circulation patterns. The sea surface temperature analysis revealed that the southwestern South Atlantic Ocean region near the coast of southeast Brazil showed strong negative association with precipitation over southeast Brazil, indicating that increased sea temperatures in this ocean region are consistent with reduced precipitation as observed in summer 2014. The circulation analysis revealed prevailing anti-cyclonic anomalies at lower levels (850 hPa) with northerly anomalies to the west of southeast Brazil, channeling moisture from the Amazon towards Paraguay, northern Argentina and southern Brazil, and drier than normal air from the South Atlantic Ocean towards the southeast region of Brazil. This circulation pattern was found to be part of a large-scale teleconnection wave train linked with the subsidence branch of the Walker circulation in the tropical east Pacific, which in turn was generated by an anomalous tropical heat source in north/northeastern Australia. A regional Hadley circulation with an ascending branch to the south of the subsidence branch of the Walker circulation in the tropical east Pacific was identified as an important component connecting the tropical and extratropical circulation. The ascending branch of this Hadley circulation in the south Pacific coincided with an identified Rossby wave source region, which contributed to establishing the extratropical component of the large-scale wave train connecting the south Pacific and the Atlantic region surrounding southeast Brazil. This connection between the Pacific and the Atlantic was confirmed with Rossby ray tracing analyses. The local circulation response was associated to downward air motion (subsidence) over Southeast Brazil, contributing to the expressive negative precipitation anomalies observed during summer 2014, and leading to a major drought event in the historical context. The analysis of atmospheric and oceanic patterns of this event helped defining a schematic framework leading to the observed drought conditions in southeast Brazil, including the involved teleconnections, blocking high pressure, radiative and humidity transport effects.

Keywords Drought · Teleconnections · Sea surface temperature · Austral summer · Precipitation · Southeast Brazil

✉ Caio A. S. Coelho
caio.coelho@cptec.inpe.br

[1] Centro de Previsão de Tempo e Estudos Climáticos (CPTEC), Instituto Nacional de Pesquisas Espaciais (INPE), Rodovia Presidente Dutra, Km 40, SP-RJ, Cachoeira Paulista, SP 12630-000, Brazil

[2] Instituto de Astronomia, Geofísica e Ciências Atmosféricas (IAG), Universidade de São Paulo (USP), Rua do Matão, 1226, São Paulo, SP 05508-090, Brazil

[3] Instituto de Recursos Naturais, Universidade Federal de Itajubá (UNIFEI), Av BPS, 1303, Itajubá, MG 37500-903, Brazil

1 Introduction

The southeast region of Brazil, here defined as the area between 15°S and 25°S and 55°W and 40°W illustrated

Published online: 15 August 2015

by the rectangle in Fig. 1a, experienced in austral summer (here defined as January–February–March) 2014 a major drought event in terms of an expressive precipitation deficit. Figure 1a shows that some areas within the here defined southeast region of Brazil experienced precipitation deficit of more than 300 mm. This event led to a number of impacts in water availability for human consumption, agricultural irrigation and hydropower production, heavily affecting water resources, food and energy production in Brazil's most populated region.

Around 70 % of Brazil's electricity is currently produced with hydropower plants, and the southeast region of Brazil concentrates a large majority of them. This fact illustrates the importance of water availability in this region for the country's electricity system, which is currently interconnected making it possible to transfer energy produced in one region to another. When water is scarce the government is forced to produce a larger than usual amount of electricity with thermal plants that burn fossil fuel to compensate the reduced production with hydropower plants. This procedure indicates that climate variability, particularly over the vastly populated region of Brazil here investigated, has an important impact in governmental actions. Understanding the observed climate variability and explaining the causes of droughts over this region is therefore fundamental to support strategic government decisions.

In a recent past, during austral summer 2001, another important drought event was experienced over the geographical southeast region of Brazil, composed by the States of São Paulo, Minas Gerais, Rio de Janeiro and Espírito Santo, causing major impacts, particularly for the energy sector. At that time the Brazilian electricity system was not fully interconnected to allow energy transfer from one region to another. The country faced a dramatic electricity crisis, forcing the population to adopt measures to reduce electricity consumption. During the austral summer 2014 drought event over the geographical southeast region of Brazil, now with a fully functioning interconnected system, the country avoided another electricity crisis. However, a water resources crisis was established. For example, São Paulo State cities including the capital city of São Paulo, with a population of around 12 million people, suffered water shortage for human consumption because the reservoirs reached extremely low levels. Coelho et al. (2015) have recently reported the expressive precipitation deficit observed during this event over a particular region of São Paulo State. The local government was forced to build a system capable of pumping water from deep reservoir levels that were never reachable in the past (Porto et al. 2014). This is another example of the importance of climate variability studies to explain anomalous conditions such as droughts, particularly for the heavily populated

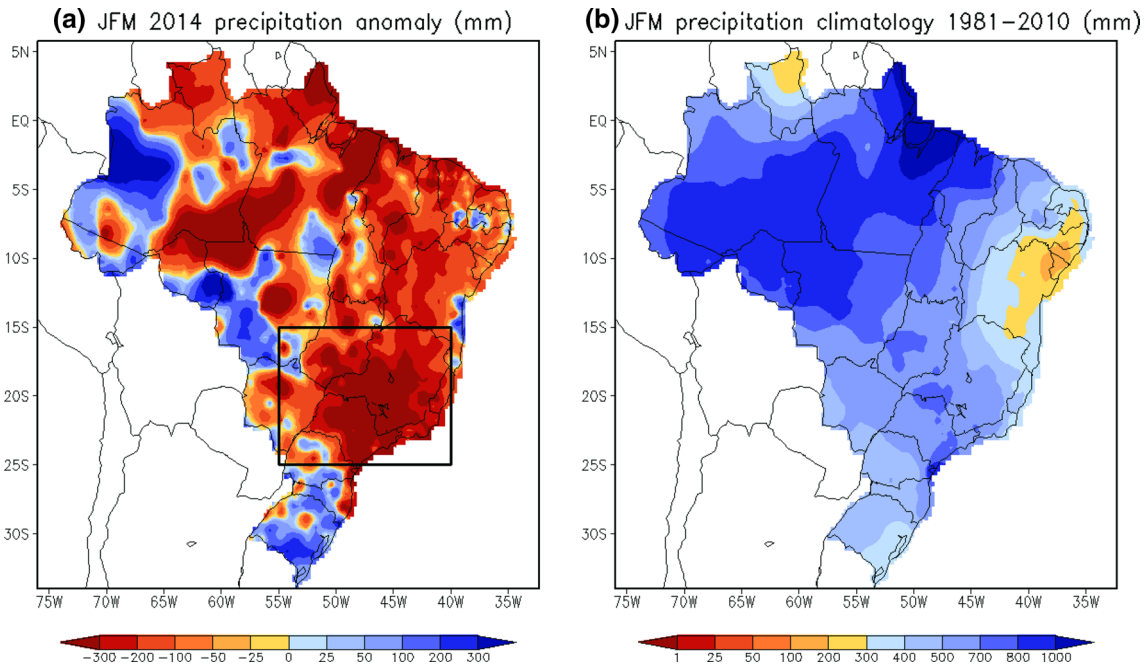

Fig. 1 **a** Austral summer (January–February–March) 2014 precipitation anomalies (mm) over Brazil with respect to **b** 1981–2010 precipitation climatology (mm). The *rectangle* in **a** defines the southeast region of Brazil (area between 15°S and 25°S and 55°W and 40°W). The precipitation data used to construct these maps is from the Brazilian network of stations maintained by the National Meteorological Service (INMET), the National Institute for Space Research (INPE) and regional meteorological centres

region of Brazil here investigated, to support future strategic government decisions.

Austral summer is the peak precipitation season over the geographical southeast region of Brazil when the largest volumes are generally experienced (Grimm 2003). This regional precipitation configuration is characterized by a northwest–southeast diagonally oriented spatial pattern with values ranging between 500 and 800 mm based on the 1981–2010 climatology as illustrated in Fig. 1b. This pattern is caused by extratropical frontal systems that reach the region and interact with tropical convection (Kousky 1979). This convection is in turn associated with tropical humidity advection from the Amazon region via the so-called low level jet (Marengo et al. 2002), a flow that surrounds the Andes Mountains towards the south/southeast direction. The diagonal precipitation configuration that extends from the Amazon to the southwestern South Atlantic, passing over the southeast region of Brazil here investigated, is known as the South Atlantic Convergence Zone (SACZ) (Kodama 1992, 1993; Herdies et al. 2002).

Climate variability over the geographical southeast region of Brazil, which is incorporated within the area defined by the rectangle in Fig. 1, has been investigated by several authors in recent years (Drumond and Ambrizzi 2005; Grimm et al. 2007; Grimm and Zilli 2009; Bombardi et al. 2013). These studies provided an outstanding background of some atmospheric and oceanic aspects related to the observed climate variability in this region. However, there is still the need for further studies to bring light into advance the understanding of mechanisms associated with the causes of droughts over this region as recently observed in 2014, particularly during the austral summer. With the aim of contributing to advance understanding the causes of the 2014 drought over the southeast region of Brazil, this paper will:

- Diagnose the observed austral summer (January–March) precipitation conditions over the southeast region of Brazil defined by the rectangle in Fig. 1a, putting the 2014 drought event recorded in this region with major impacts in historical context.
- Analyse the observed oceanic and atmospheric circulation and investigate regional mechanisms and possible oceanic and atmospheric teleconnection patterns associated with the 2014 austral summer drought over the southeast region of Brazil.
- Propose a schematic framework for the occurrence of the austral 2014 summer drought over the southeast region of Brazil.

The manuscript is organized as follows. Section 2 places the 2014 drought event in historical context. Section 3 investigates the large-scale dynamics of this drought event including an analysis of the relationship between southeast Brazil precipitation and large-scale ocean and atmospheric conditions. Section 4 describes regional vertical anomalous profiles and the role of the high pressure anomaly over the warm south Atlantic in maintaining favourable drought conditions over southeast Brazil during the austral summer 2014. Section 5 presents a Rossby wave analysis for the 2014 austral summer drought event. Finally, Sect. 6 presents a summary with concluding remarks.

2 The 2014 southeast Brazil drought event in historical context

The investigation of the 2014 drought event in historical context was performed using 1961–2014 precipitation time series from the observed meteorological station network from the Center for Weather Forecast and Climate Studies (CPTEC) of the Brazilian National Institute for Space Research (INPE), the Brazilian National Meteorological Service (INMET) and regional meteorological offices around Brazil. All available station data were interpolated using Kriging to a regular 0.25° grid in latitude and longitude. For the analysis over the southeast region of Brazil, the interpolated data was averaged over the area between 15°S and 25°S and 55°W and 40°W illustrated by the rectangle in Fig. 1a. This is the same data source recently used by Coelho et al. (2015) for diagnosing the expressive precipitation deficit observed over the State of São Paulo, Brazil. The reliability of the used dataset was checked by comparison with the dataset prepared by the Global Precipitation Climatology Centre (GPCC, Schneider et al. 2014) and finding a correlation of 0.89 between the two datasets. Such high correlation provides confidence that the used dataset represents appropriately the observed inter-annual austral summer precipitation variability during the period 1961–2014 over the investigated southeast region of Brazil.

Figure 2 shows the area average austral summer (January–February–March) 1961–2014 precipitation anomaly time series over the southeast region of Brazil. The austral summer of 2014 stands out with the largest negative precipitation anomaly of −249.7 mm with respect to the 1981–2010 climatological mean value for the region (574.3 mm), illustrating the expressive magnitude and uniqueness of the 2014 austral summer drought event in the investigated record. In fact, Fig. 2 shows that the region experienced important precipitation deficits in the last 3 years. Examining the historical time series of Fig. 2 one can notice that the region experienced a predominant period of precipitation excess between 1961 and 1967, followed by a period of precipitation deficit between 1968 and 1978, returning to period predominated by precipitation excess between 1979 and 1997, and finally a period predominated by

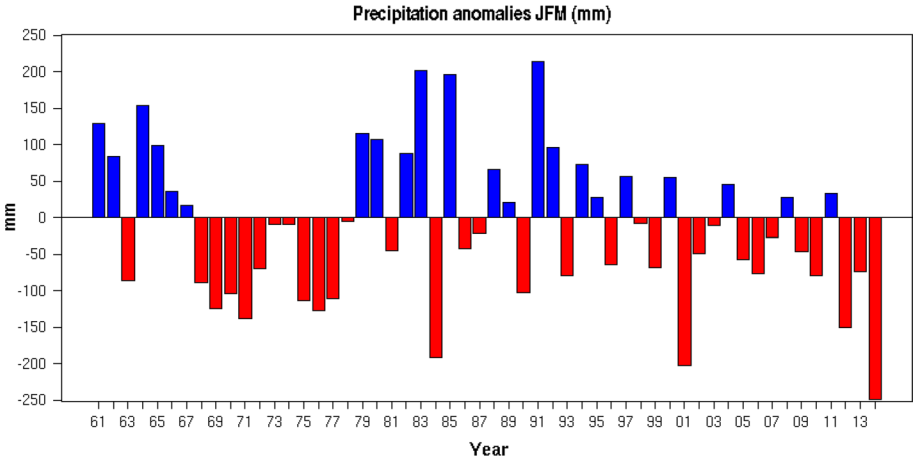

Fig. 2 Area average austral summer (January–February–March) 1961–2014 precipitation anomaly time series (*colour bars*) expressed in mm over the southeast region of Brazil defined by the *rectangle* in Fig. 1a. The precipitation data used to construct this time series is from the Brazilian network of stations maintained by INMET, INPE and regional meteorological centres. Anomalies are computed with respect to the 1981–2010 climatological mean for the region of 574.3 mm. Years with positive precipitation anomalies (i.e. precipitation excess) are shown in *blue* and those with negative precipitation anomalies (i.e. precipitation deficit) are shown in *red*

precipitation deficit between 1998 and 2014. This indicates that not only the last 3 years were anomalously dry, but since 1998 (i.e. over the last 17 years) the region is experiencing important precipitation deficit. Over these last predominantly dry years 2001 stands out as the second driest year with negative precipitation anomalies of −202.1 mm. This expressive anomaly also highlights the magnitude of the drought experienced in the region in 2001 with major impacts as described in Sect. 1.

The percentual and standardized precipitation anomaly calculations revealed that during the 2014 austral summer only 56.5 % of the 1981–2010 climatological mean of 574.3 mm was observed over the southeast region of Brazil, representing an impressive percentual deficit anomaly of 43.5 %, and a standardized precipitation anomaly of −2.54 standard deviations. The standardized precipitation anomaly is unitless (i.e. it does not have physical unit) because it was obtained dividing the 2014 precipitation anomaly of Fig. 2 (expressed in mm) by the climatological 1981–2010 standard deviation of 98.4 mm. In 2001 only 64.8 % of the climatological mean of 574.3 mm was observed, representing the second largest percentual deficit anomaly of 35.2 % in this historical record, and a standardized precipitation anomaly of −2.05 standard deviations. Both austral summer 2014 and 2001 stand out with the two smallest standardized precipitation anomalies indicating that the observed precipitation deficits over the southeast region of Brazil were more than twice the climatological standard deviation. These results highlight these two events as extreme cases placed well into the tail of the precipitation distribution for this region. The following sections will focus the analysis on the 2014 event.

3 Large-scale dynamics

This session aims to investigate the relationship between southeast Brazil precipitation and large-scale ocean and atmospheric patterns in order to identify possible forcing mechanisms associated to droughts over the southeast region of Brazil, with a particular focus on the 2014 drought event. Climate variability on seasonal time scales has been documented to be related by slowly varying boundary conditions (Charney and Shukla 1981; Branković et al. 1994). Sea surface temperature is generally considered a key slowly varying parameter for understanding climate anomalies. In this context, Fig. 3a shows (in colours) the simultaneous Spearman rank correlation between 1961 and 2014 austral summer (January–February–March) precipitation over the southeast region of Brazil and sea surface temperatures (Rayner et al. 2003). The rank-correlation is used because it is potentially better suited for representing non-linearity that may exist in these relationships. A pattern of negative correlation coefficients statistically significant at the 15 % level, with values between −0.2 and −0.6, stands out over the South Atlantic Ocean, around 30°S, near the south and southeast coast of Brazil. This result indicates that during this 54-year period between 4 and 36 % of the austral summer precipitation variability over the southeast region of Brazil is related to sea surface temperature variability over this South Atlantic Ocean region. The negative sign of the correlation coefficients indicate consistency between increased sea surface temperatures over this ocean region and reduced precipitation over the southeast region of Brazil. Conversely, decreased sea surface temperatures

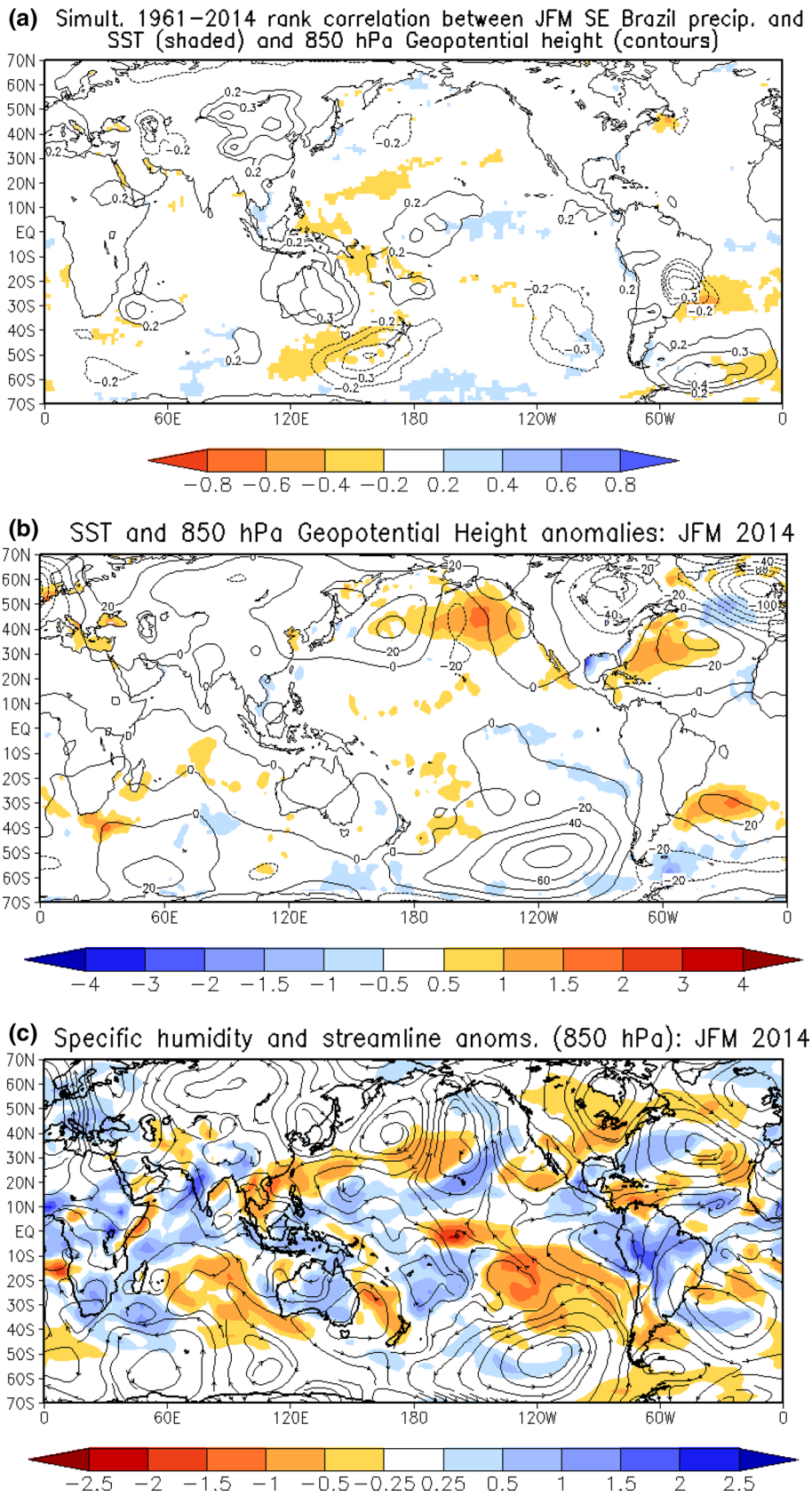

Fig. 3 **a** Simultaneous spearman rank correlation between 1961 and 2014 austral summer (January–February–March) area average precipitation over the southeast region of Brazil defined by the *rectangle* in Fig. 1a and sea surface temperatures (*colours*) and 850 hPa geopotential height (*countours*). Only statistically significant correlation coefficients at the 15 % level are shown. Austral summer 2014: **b** sea surface temperature in °C (*colours*) and 850 hPa geopotential height in m (*contours*) anomalies and **c** specific humidity in g kg^{-1} (*colours*) and circulation (*streamline*) anomalies at 850 hPa. Anomalies are computed with respect to the 1981–2010 climatological period

over this ocean region are consistent with increased precipitation over the southeast region of Brazil. These results suggest that austral summer precipitation variability over the southeast region of Brazil is connected to regional sea surface temperature variability over the South Atlantic Ocean.

In order to investigate the relationship between precipitation variability over the southeast region of Brazil and the large-scale atmospheric pattern, Fig. 3a also shows (with contour lines) simultaneous Spearman rank correlation between 1961 and 2014 austral summer (January–February–March) precipitation over the southeast region of Brazil and 850 hPa geopotential height (Kalnay et al. 1996). The contours in Fig. 3a show a pattern of negative correlations over the southeast region of Brazil and southeast Pacific Ocean near the west coast of South America, and positive correlations over the South Atlantic Ocean. This result indicates that when atmospheric pressure is increased over the southeast region of Brazil and southeast Pacific Ocean near the west coast of South America, and decreased over the South Atlantic Ocean, the southeast region of Brazil tend to have reduced precipitation. This is the atmospheric pattern favourable for the establishment of drought conditions over the southeast region of Brazil, which is under influence of high atmospheric pressure, a condition unfavourable for cloud development and precipitation. Conversely when atmospheric pressure is reduced over the southeast region of Brazil and southeast Pacific Ocean near the west coast of South America, and increased over the South Atlantic Ocean, the southeast region of Brazil tends to have increased precipitation.

Figure 3b shows the observed austral summer (January–February–March) 2014 sea surface temperatures (colours) and 850 hPa geopotential height anomalies (contours). The South Atlantic stands out with positive sea surface temperature anomalies between 0.5 and 2 °C around 30°S near the southeast coast of Brazil. This ocean pattern is consistent with Fig. 3a that shows negative correlation between sea surface temperatures over this ocean region and precipitation over the southeast region of Brazil during the austral summer. As illustrated in Figs. 1a and 2, the southeast region of Brazil indeed experienced expressive precipitation deficit during the austral summer 2014, leading to drought conditions. These conditions were linked to the establishment of two anomalous high pressure centres and one anomalous low pressure centre in the vicinities of South America, as illustrated by the 850 hPa geopotential height anomalies in Fig. 3b. Positive geopotential height anomalies are indicative of anomalous high pressure and negative geopotential high anomalies are indicative of anomalous low pressure. The two anomalous high pressure centres were established over the southeast Pacific Ocean near the west coast of South America, and over the Atlantic Ocean around 30°S (over the region presenting positive sea surface temperature anomalies). The anomalous low pressure centre was established over the South Atlantic Ocean.

Figure 3c shows austral summer 2014 specific humidity (colours) and circulation anomalies (stream lines) at 850 hPa. The circulation pattern reproduces anticyclonic (high pressure) anomalies in the Pacific and Atlantic, in the vicinities of South America, and cyclonic (low pressure) anomalies in the South Atlantic. This figure indicates that the anticyclonic anomaly over the Atlantic extends westwards and reaches the southeast region of Brazil where drought conditions were established. The specific humidity pattern shows positive anomalies in the Amazon region and negative anomalies in southern South America. The figure also suggests that an anomalous northerly flow is capable of transporting humidity from the Amazon towards Paraguay, Uruguay and the south region of Brazil in a similar configuration as described by Nogués-Paegle and Mo (1997). This circulation and humidity pattern is consistent with the anomalous precipitation pattern observed during austral summer 2014 (Fig. 1a), with positive precipitation anomalies over south and northwest of Brazil (Espinoza et al. 2014). Over the southeast region of Brazil, where drought conditions were observed, Fig. 3c also shows that the anticyclonic circulation favoured the transport of negative specific humidity anomalies from the Atlantic Ocean towards this region.

The simultaneous Spearman rank correlation between 1961 and 2014 austral summer precipitation over the southeast region of Brazil and 200 hPa geopotential height shown in Fig. 4a (contours) highlights a u-shaped wave-like pattern. This pattern is characterised by two symmetric positive correlation centres about the equator in both hemispheres over the eastern Pacific (around 130°W), followed by a small negative correlation centre over the southeast Pacific Ocean near the southwest coast of South America, a positive correlation centre over the South Atlantic Ocean, a negative correlation centre around 35°S over the South Atlantic and in the vicinities of the south region of Brazil, and a positive correlation centre near the equator, over the northeast region of Brazil. This result indicates that when upper level atmospheric pressure is reduced over the eastern equatorial Pacific (around 130°W), South Atlantic Ocean and northeast region of Brazil, and increased over the southeast Pacific Ocean near the southwest coast of South America and the South Atlantic around 35°S in the vicinities of the south region of Brazil, the southeast region of Brazil tend to experience reduced precipitation. This upper level wave-like pattern is suggestive of a teleconnection, presenting a predominantly barotropic structure with the lower level (850 hPa) pattern shown in Fig. 3a. The barotropic structure is identified by the same sign for the correlation coefficients in upper (Fig. 4a) and

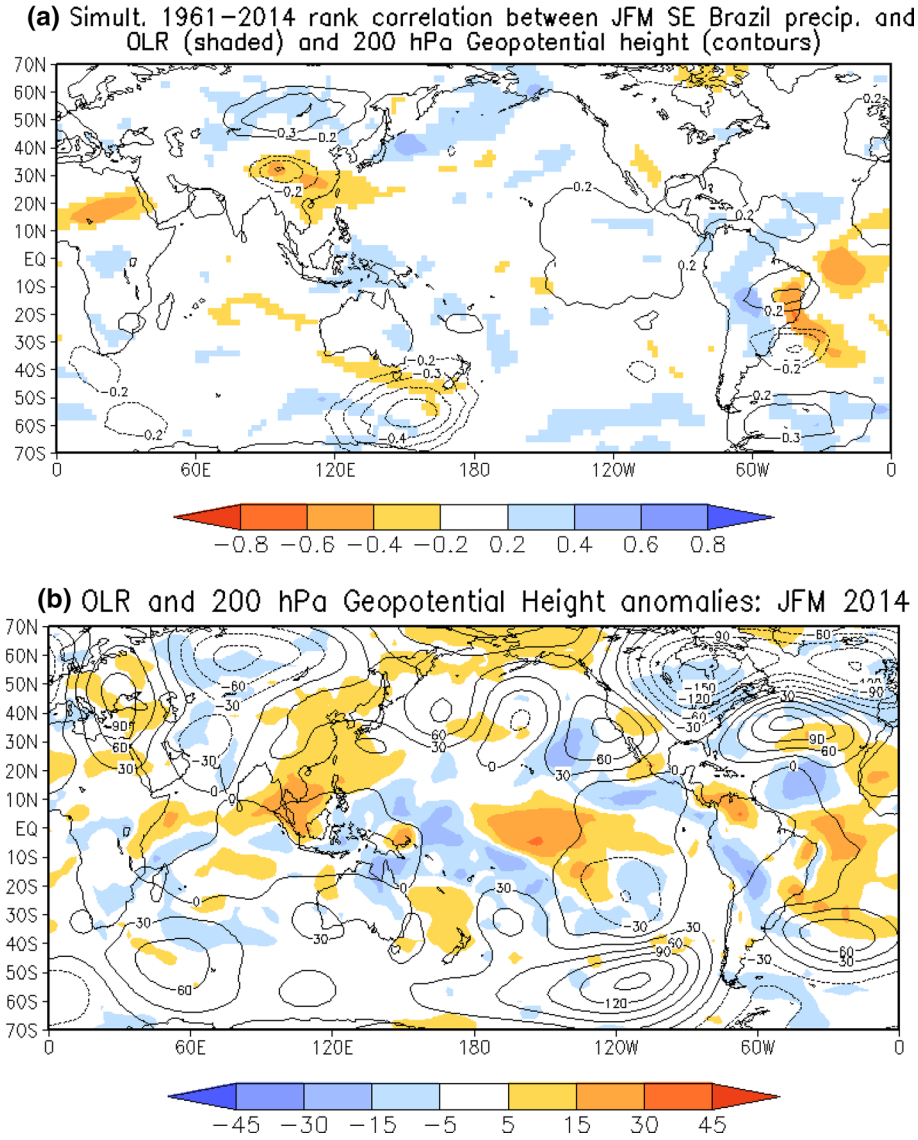

Fig. 4 **a** Simultaneous spearman rank correlation between 1961 and 2014 austral summer (January–February–March) area average precipitation over the southeast region of Brazil defined by the *rectangle* in Fig. 1a and outgoing longwave radiation (*colours*) and 200 hPa geopotential height (*contours*). Only statistically significant correlation coefficients at the 15 % level are shown. **b** Austral summer 2014 outgoing longwave radiation in W m^{-2} (*colours*) and 200 hPa geopotential height in metres (*contours*) anomalies. Anomalies are computed with respect to the 1981–2010 climatological period

lower (Fig. 3a) levels particularly over the southeast Pacific Ocean near the west coast of South America and the South Atlantic Ocean. This pattern is consistent for the establishment of drought conditions over the southeast region of Brazil, with high atmospheric pressure conditions over this region, preventing cloud formation and precipitation. Conversely when upper level atmospheric pressure is increased over the eastern equatorial Pacific (around 130°W), South Atlantic Ocean and northeast region of Brazil, and reduced over the southeast Pacific Ocean near the southwest coast of South America and the South Atlantic around 35°S and in the vicinities of the south region of Brazil, the southeast region of Brazil tends to experience increased precipitation.

Figure 4b shows austral summer 2014 outgoing longwave radiation and 200 hPa geopotential height anomalies. Positive outgoing longwave radiation anomalies are noticed over the southeast region of Brazil, indicating reduced cloudiness, in consistency with the reduced observed precipitation and the negative correlations shown in Fig. 4a (contours) over this region. Over the equatorial Pacific northeast of Australia (around 160°E) negative outgoing longwave radiation anomalies are noticed, indicating the presence of a deep cloud structure acting as a tropical heat source. To the east of this tropical heat source positive outgoing longwave radiation anomalies are observed over the equatorial Pacific (around 150°W), indicating the absence of clouds over this region. This tropical pattern is explained by a Walker circulation cell with upward vertical motion (i.e. favourable conditions for convection and cloud formation) over the region of negative outgoing longwave radiation around 160°E, and downward vertical motion (i.e. subsidence conditions suppressing convection and cloud formation) over the region of positive longwave radiation around 150°W.

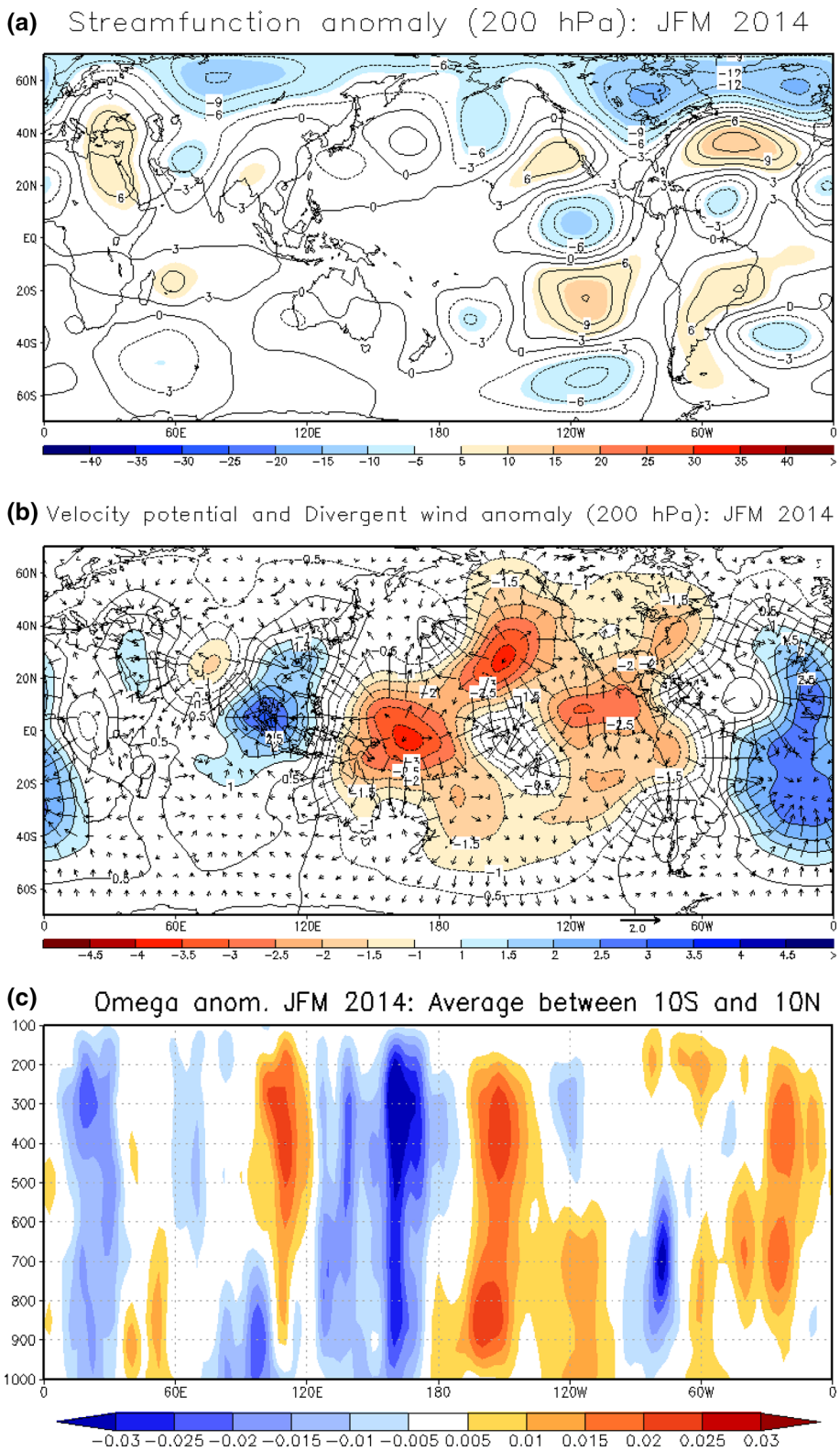

Fig. 5 Austral summer 2014: **a** streamfunction anomalies in 5×10^6 m^2 s^{-1}, **b** velocity potential anomalies in 10^6 m^2 s (*contours* and *colours*) and divergent wind anomalies in m s^{-1} (*vectors*), and **c** longitudinal cross-session with average vertical velocity (*omega*) anomalies between 10°S and 10°S in Pa s^{-1}. Anomalies are computed with respect to the 1981–2010 climatological period

The 200 hPa geopotential height anomalies of Fig. 4b shows a u-shaped wave-like pattern placed to the east of the maximum positive outgoing longwave radiation anomalies in the equatorial Pacific. This wave-like teleconnection pattern in the southern hemisphere, which is consistent with the previous analysis shown in Fig. 4a, is linked to the upper level convergence and downward vertical motion of the Walker cell described above. This teleconnection

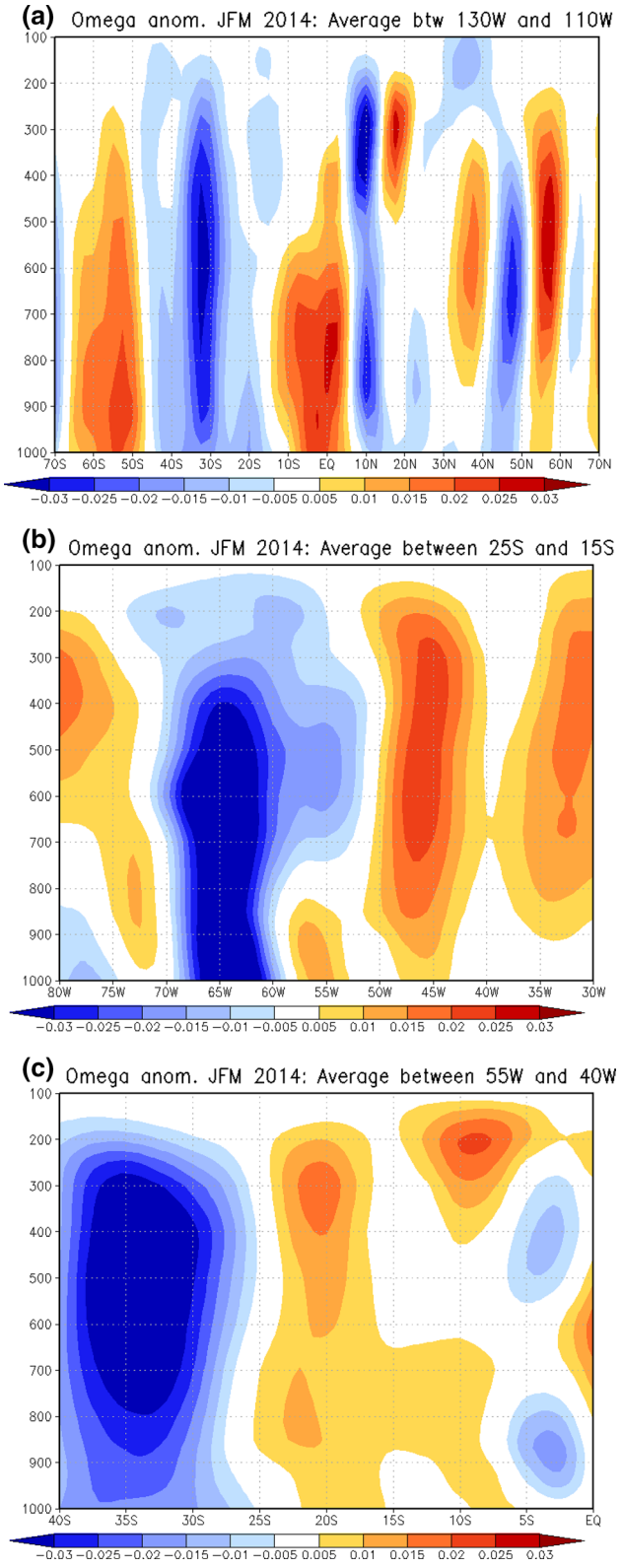

◀ **Fig. 6** Austral summer (January–February–March) 2014: **a** latitudinal cross-session with average vertical velocity (*omega*) anomalies between 130°W and 110°W in Pa s^{-1}, **b** longitudinal cross-session with average vertical velocity (*omega*) anomalies between 15°S and 25°S in Pa s^{-1} and **c** latitudinal cross-session with average vertical velocity (*omega*) anomalies between 55°W and 40°W in Pa s^{-1}. Cross-sessions are from 1000 to 100 hPa. Anomalies are computed with respect to the 1981–2010 climatological period

pattern is composed by two equatorially symmetric anomalous low pressure centres around 120°W, followed by an anomalous high pressure centre over the southeast Pacific Ocean near the southwest coast of South America, an anomalous low pressure centre over the South Atlantic Ocean, and an anomalous high pressure centre around 40°S over the South Atlantic and in the vicinities of the south and southeast regions of Brazil. Figure 4b shows a similar and symmetric teleconnection pattern in the northern hemisphere over North America. These symmetric u-shaped wave-like patterns are even more visible in Fig. 5a that shows 200 hPa streamfunction anomaly (a variable that represents the rotational component of the atmospheric flow) for austral summer 2014. The u-shaped wave-like pattern with alternated anomalous low and high pressure centres in the southern hemisphere has a predominantly barotropic vertical structure as earlier identified in Figs. 3a and 4a, with high pressure anomalies over the Pacific and Atlantic ocean in the vicinities of South America and a low pressure anomaly in the south Atlantic.

Figure 5b shows 200 hPa velocity potential and divergent wind vector anomaly for austral summer 2014, which represents the non-rotational component of the atmospheric flow. Near the equator one can identify a pattern of divergent winds around 160°E and convergent winds around 150°W over the Pacific. This pattern is consistent with the outgoing longwave radiation anomalies shown in Fig. 4b and supports the earlier described Walker circulation with an ascending branch around 160°E and a descending branch around 150°W. This circulation is illustrated by the longitudinal vertical velocity anomalies cross-section (average between 10°S and 10°S) shown in Fig. 5c. Negative vertical velocity anomalies (ascending motion) are noticed around 160°E and positive vertical velocity anomalies (descending motion or subsidence) are noticed around 150°W.

4 Regional vertical profiles and the role of the south Atlantic anomalous high pressure

Figure 6a shows the austral summer 2014 latitudinal cross-session, from 1000 to 100 hPa, with average vertical velocity (omega) anomalies between 130°W and 110°W (around the initial longitudinal range where the u-shaped wave-like pattern was previously identified). Positive anomalies are noticed between 5°N and 10°S over the equatorial Pacific, indicating anomalous descending vertical motion (subsidence preventing cloud formation and precipitation) over this region. Negative anomalies are noticed between 15°S

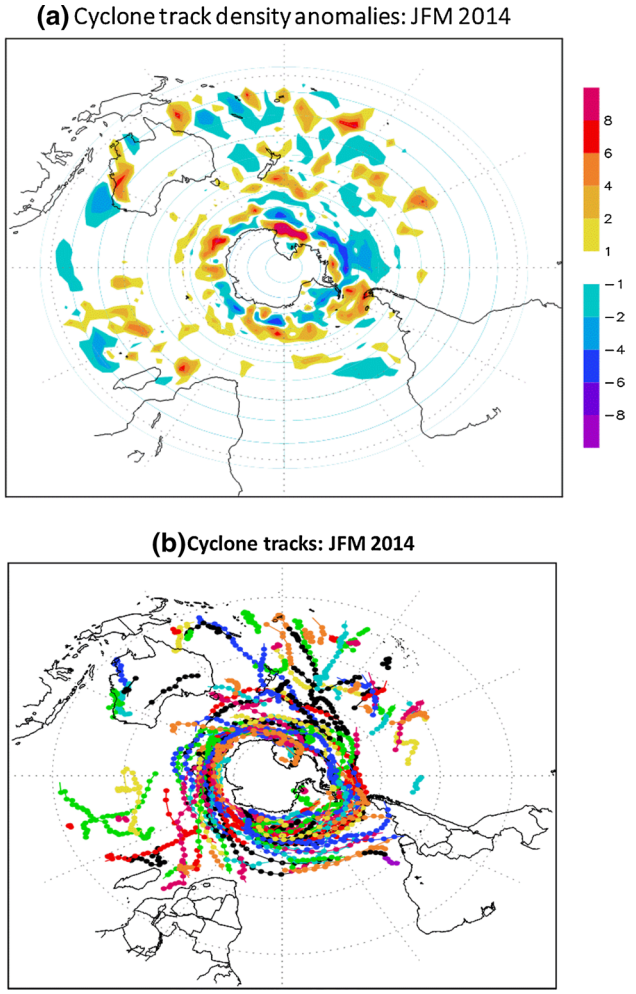

Fig. 7 **a** Cyclone tracks density anomalies during austral summer 2014 with respect to 1980–2012 period. **b** Cyclone tracks during the austral summer 2014. Tracks were computed using six-hourly mean sea level pressure (Kalnay et al. 1996) as described in Reboita et al. (2014)

and 45°S, indicating anomalous ascending vertical motion (favourable conditions for convection) over this region. These vertical velocity anomalies characterize a regional Hadley circulation cell, connecting the tropical and extra-tropical circulation, with an ascending branch to the south of the subsidence branch around the equator.

Figure 6b shows the austral summer 2014 longitudinal cross-session, from 1000 to 100 hPa, with average vertical velocity (omega) anomalies between 15°S and 25°S (the northernmost and southernmost latitudes of the rectangle defining the southeast region of Brazil in Fig. 1a). Positive anomalies are noticed between 50°W and 30°W over the southeast region of Brazil and Atlantic Ocean, indicating anomalous descending vertical motion (subsidence preventing cloud formation and precipitation) over these regions. Negative anomalies are noticed between 70°W and 60°W over Paraguay, southern Bolivia and northern Argentina, indicating anomalous ascending vertical motion (favourable conditions for convection) over these regions. These vertical velocity anomalies characterize a regional Walker circulation cell, connecting the circulation of the southeast region of Brazil with western neighboring countries.

Figure 6c shows the austral summer 2014 latitudinal cross-session, from 1000 to 100 hPa, with average vertical velocity (omega) anomalies between 55°W and 40°W (the westernmost and easternmost longitudes of the rectangle defining the southeast region of Brazil in Fig. 1a). Positive anomalies are noticed between 5°S and 25°S over the northeast and southeast regions of Brazil, indicating anomalous descending vertical motion (unfavourable conditions for cloud formation and precipitation) over these regions. Negative anomalies are noticed between 28°S and 40°S over the Atlantic Ocean and a large portion of South Brazil, indicating anomalous ascending vertical motion (favourable conditions for convection) over these regions. These vertical velocity anomalies characterize a regional Hadley circulation cell, connecting the circulation of the southeast region of Brazil here investigated with south Brazil and neighboring Atlantic Ocean.

The vertical velocity anomalies identified in Fig. 6 are in accordance with the observed precipitation deficit over the southeast region of Brazil (Figs. 1, 2) and the outgoing longwave radiation anomaly pattern shown in Fig. 4b. This accordance is realised by noticing that negative precipitation anomalies and/or positive outgoing longwave radiation anomalies are observed over the regions with positive omega anomalies (i.e. prevailing descending motion), and negative outgoing longwave radiation anomalies are observed over the regions with negative omega anomalies (i.e. prevailing ascending motion).

As described in Sect. 3 during austral summer 2014 a high pressure centre at lower levels (850 hPa) was established around 35°S, over a warm South Atlantic Ocean region. The high pressure centre acts as an atmospheric barrier blocking the passage or diverting the trajectory of frontal system away from the southeast region of Brazil. This configuration is illustrated in Fig. 7, which shows cyclone tracks density anomalies and cyclone tracks during austral summer 2014 [see Reboita et al. (2014) and references therein for further information on how tracks density anomalies and tracks are calculated]. Cyclones are used here as tracers for frontal systems. Negative cyclone tracks density anomalies are found over the South Atlantic Ocean near the coast of the southeast region of Brazil (Fig. 7a), with absence of cyclone tracks in this region (Fig. 7b). In fact this figure reveals that cyclone tracks were preferentially concentrated in higher latitudes in the South Atlantic. With the absence of cyclones and associated frontal systems moving to the north, a direct consequence was that during austral summer 2014 SACZ episodes were rarely

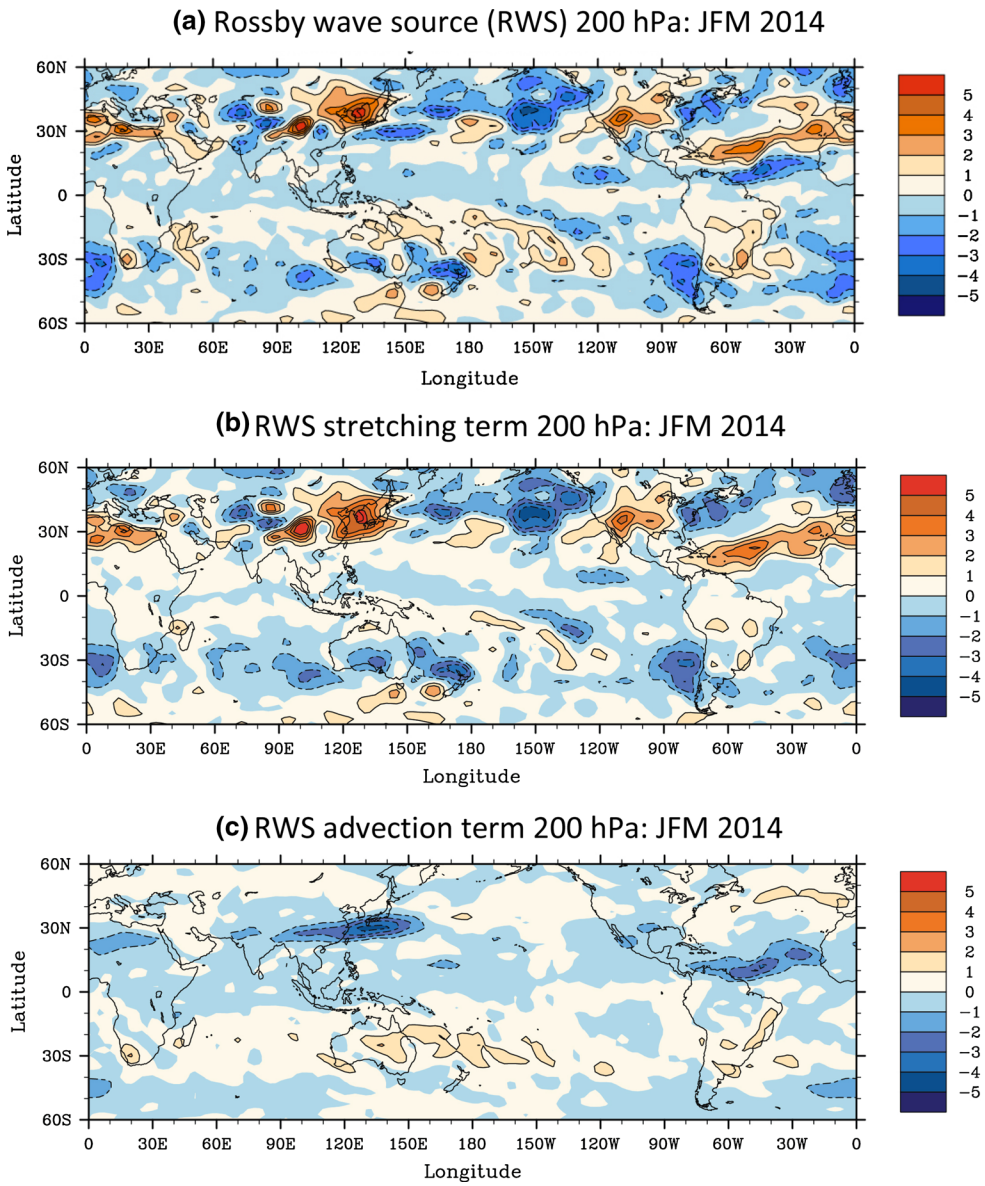

Fig. 8 Austral summer 2014: **a** Rossby wave source (RWS), **b** vortex stretching term of RWS and **c** advection term of RWS, all at 200 hPa in 10^{-11} s^{-2}

configured and the southeast region of Brazil experienced reduced precipitation. Clear sky conditions over the high pressure centre (around 35°S) in the South Atlantic were also likely to have helped maintain the anomalously warm sea surface temperatures in this ocean region via shortwave solar radiation reaching the surface.

5 Rossby wave analysis

In order to further understand the large-scale atmospheric teleconnection diagnosed in Sect. 3 this section performs an upper level (200 hPa) Rossby wave analysis during the 2014 austral summer. Rossby wave propagation is recognized as a key atmospheric mechanism for explaining atmospheric teleconnections. The first part of this analysis consisted in computing the so-called Rossby Wave Source (RWS, Sardeshmukh and Hoskins 1988) given by

$$\mathrm{RWS} = \underset{(S1)}{-\mathrm{V}_\chi \cdot \nabla(\zeta + \mathrm{f})} \underset{(S2)}{- (\zeta + \mathrm{f})\nabla \cdot \mathrm{V}_\chi} \quad (1)$$

where V_χ is the non-rotational (divergent) wind vector component, ζ is the relative vorticity and f is the Coriolis parameter. Equation 1 shows that RWS is written as the sum of two terms: S1 which represents the absolute vorticity (ζ + f) advection by the divergent flow and S2 which represents vortex stretching.

Figure 8 shows the 200 hPa Rossby wave source and corresponding vortex stretching and advection terms for the austral summer 2014. Positive values in Fig. 8a identify Rossby wave source regions, while negative values identify Rossby wave sink regions. Figure 8a shows that the central Pacific, around

30°S, and between 150°W and 110°W, appears as an important Rossby wave source region. This Rossby wave source region in the Pacific coincides with the ascending branch of the Hadley circulation discussed in Sect. 4 (Fig. 6a), where a centre of negative outgoing longwave radiation was observed (Fig. 4b). The meridional Hadley cell illustrated in Fig. 6, with ascending vertical motion around 30°S and descending vertical motion around the equator, connects the tropical and extra-tropical circulation. The clouds formed in the central Pacific around 30°S are characterized as extra-tropical heat sources capable of exciting Rossby waves leading to remote responses in consistency with the identified Rossby wave source region in the central Pacific (Fig. 8a). The vortex stretching (Fig. 8b) is the term that contributes the most for the Rossby wave source (Fig. 8a). The magnitude of the advection term (Fig. 8c) is generally much reduced when compared to the magnitude of the vortex stretching term (Fig. 8b).

Now that a Rossby wave source region was identified in the Pacific the next step is to investigate the trajectory followed by the waves generated by this source. The linearized non-divergent barotropic vorticity equation, with solution of the form exp[i(kx + ly − ωt)], leads to the following dispersion relation

$$\omega = \bar{U}k - \frac{\beta_* k}{K^2}, \tag{2}$$

where ω is the wave frequency,

$$\beta_* = \frac{df}{dy} - \frac{\partial^2 \bar{U}}{\partial y^2} \tag{3}$$

is the meridional vorticity gradient, $K = (k^2 + l^2)^{1/2}$ is the total wave number, with k and l being the zonal and meridional wave numbers, respectively, y is the meridional spatial coordinate and $\bar{U}$ is the zonal flow.

For stationary Rossby waves, k is constant along the trajectory and ω = 0. From Eq. (2) it follows that the total wave number for stationary Rossby waves (K_s) is given by

$$K = K_s = \left(\frac{\beta_*}{\bar{U}}\right)^{1/2} \tag{4}$$

From Eq. (4) one can see that stationary Rossby waves are only possible for westerly flow (i.e. positive $\bar{U}$) and for regions where the meridional vorticity gradient β_* is positive.

Figure 9a shows the 200 hPa stationary wave number (K_s) for austral summer 2014. The 200 hPa zonal wind $\bar{U}$ and meridional vorticity gradient β_* used in Eq. (4) to compute the stationary wave number (K_s) are shown in Fig. 9b, c, respectively. Figure 9b shows that equatorial regions over Africa, the Indian Ocean, the Maritime Continent and northwest South America present easterly zonal flow and are therefore unfavourable regions for stationary Rossby wave propagation. The subtropical and polar jets in the Southern Hemisphere with marked westerly zonal winds between 25°S and 65°S appear as important potential regions for Rossby wave propagation. Figure 9c shows a few regions, most notably over Europe, Asia and the Atlantic, with negative meridional vorticity gradient β_*, which are therefore unfavourable for stationary Rossby wave propagation. Two latitudinal bands in the Southern Hemisphere, around 30°S and 50°S where the subtropical and polar jets are normally observed, appear presenting local maxima positive meridional vorticity gradient, being potential regions for Rossby wave propagation.

Hoskins and Ambrizzi (1993) studied the trajectories followed by Rossby waves and derived an expression for the preferential ray path propagation, which is given by:

$$r = \frac{K_s^2}{\left(k\frac{dK_s}{dy}\right)} \tag{5}$$

Equation (5) shows that from the global distribution of the stationary wave number (K_s) it is possible to identify preferential Rossby wave trajectories. The numerical solution for the equations

$$\frac{dx}{dt} = u_g \quad \text{and} \quad \frac{dy}{dt} = v_g, \tag{6}$$

where the zonal and meridional components of the group velocity are

$$(u_g, v_g) = \left(\frac{\partial \omega}{\partial k}, \frac{\partial \omega}{\partial l}\right) = \left(c + \frac{2\beta_* k^2}{K^4}, \frac{2\beta_* kl}{K^4}\right) \tag{7}$$

and c = ω/k is the phase speed in the zonal (x) direction, using a second order Runge–Kutta scheme for an initial position (x_o, y_o), total wave number (K) and frequency (ω), results in the so-called Rossby wave ray tracing, which represents the Rossby wave ray path propagation trajectory. Additionally, the relationship between the zonal wave number k and the total wave number K given by k = K/a is required, where a is the Earth's radius.

Figure 9a shows the Rossby wave tracing computed using the numerical scheme developed by Yang and Hoskins (1996) for total wave number K = 3 for an initial point located at 135°W, 30°S (black curve) and for another initial point located at 130°W, 30°S (blue curve) for stationary waves (i.e. ω = 0). The trajectories have an initial southeast propagation towards higher latitudes in the southern hemisphere, reaching the latitude around 55°S around the southern tip of South America. After this point the wave is refracted towards the tropical region. These two initial points were located in the region earlier identified in Fig. 8a as an important Rossby wave source region. These ray tracing curves illustrate the extra-tropical teleconnection between the Pacific and the Atlantic

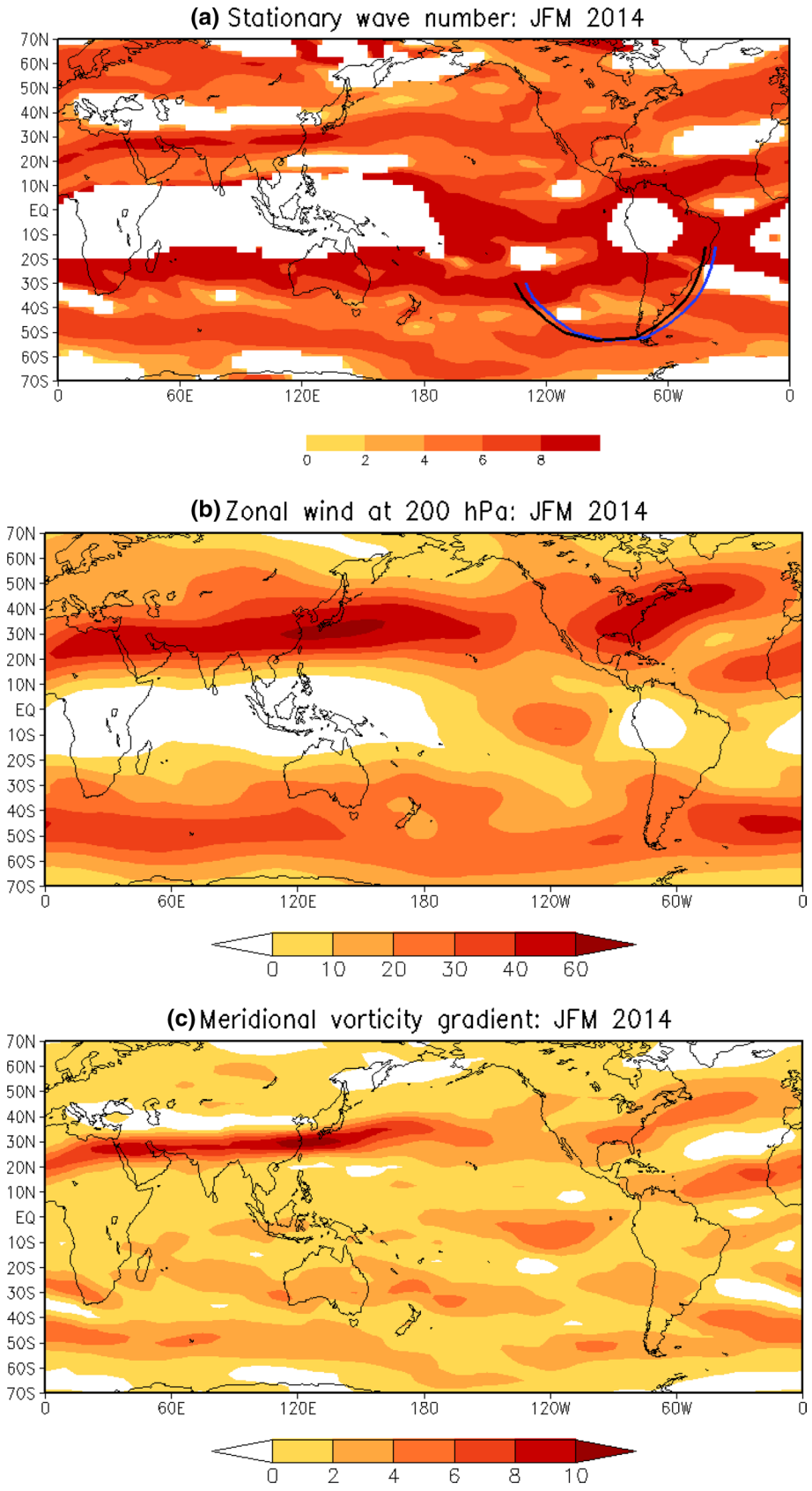

Fig. 9 Austral summer (January–February–March) 2014: **a** stationary wave number (K_s), **b** zonal wind at 200 hPa (m s^{-1}) and **c** meridional vorticity gradient (10^{-11} s^{-1} m^{-1}). The *black curve* in **a** is the Rossby wave tracing for wave number K = 3 with an initial point located at 135°W, 30°S. The *blue curve* in **a** is the Rossby wave tracing for wave number K = 3 with an initial point located at 130°W, 30°S

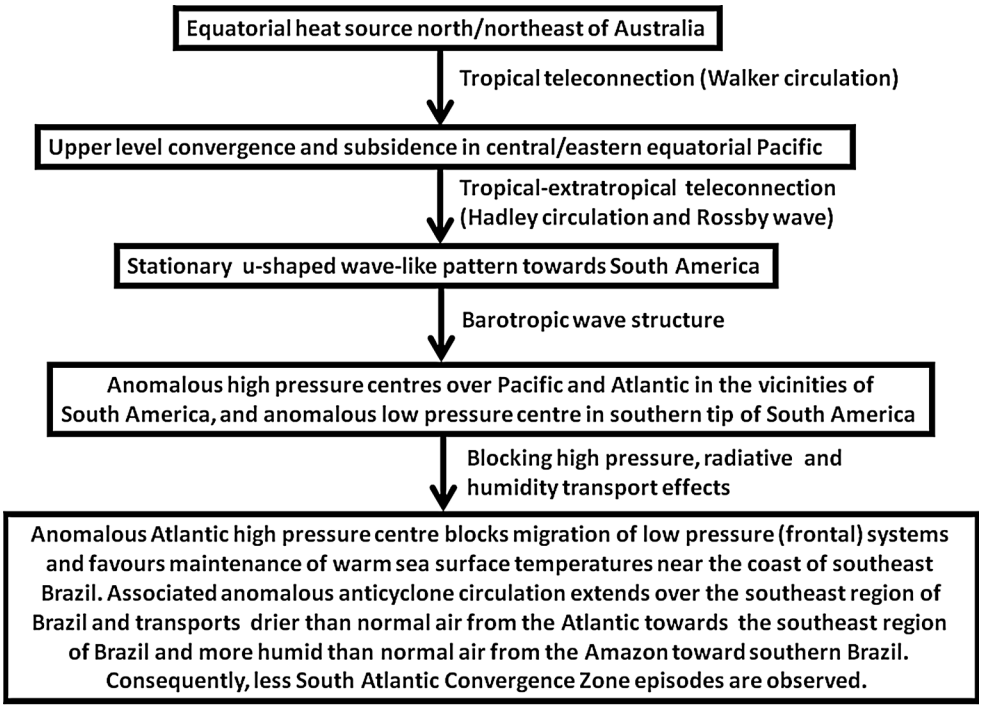

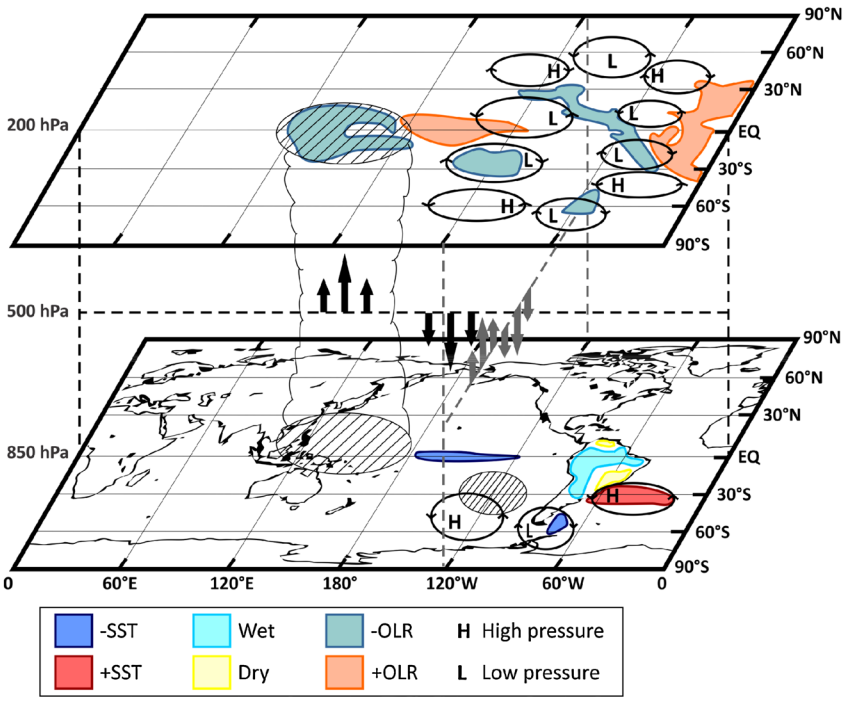

Fig. 10 Schematic framework for the occurrence of the 2014 austral summer drought over southeast Brazil with the corresponding illustrative picture

through stationary Rossby wave and is in accordance with the earlier identified wave train of Fig. 4b, resulting in an anomalous high pressure centre over the Atlantic surrounding southeast Brazil where the precipitation deficit was observed during the 2014 austral summer. A similar teleconnection between the Pacific and southeast Brazil was reported by Grimm and Silva Dias (1995).

6 Conclusions

This paper investigated the atmospheric and oceanic conditions during a major austral summer drought event manifested during January–February–March 2014 over the southeast region of Brazil, with the aim of advancing the understanding of mechanisms associated with the causes of

this drought. The particular question of interest here was: what were the atmospheric and ocean conditions capable of generating the observed drought conditions over the southeast region of Brazil during austral summer 2014? In order to answer this question, diagnostics of historical precipitation records, as well as analysis of the observed oceanic and atmospheric circulation patterns during this drought event, and the investigation of possible teleconnection patterns associated with this austral summer drought over the southeast region of Brazil, were performed. The results are summarised in Fig. 10 that shows a proposed schematic framework (with an illustrative picture) for the occurrence of the 2014 austral summer drought over the southeast region of Brazil. The proposed mechanisms are described below.

An Equatorial heat source located in the north/northeast of Australia, resulting from anomalous convective activity, induces a tropical teleconnection via a zonal Walker circulation cell. This teleconnection is manifested by ascending vertical motion over the region where the heat source is located and descending vertical motion (subsidence) to the east of the heat source in central/eastern equatorial Pacific. The tropical and extratropical circulation is connected by a meridional Hadley circulation cell in the central/eastern equatorial Pacific. This cell is characterized by ascending vertical motion over a region identified as an important Rossby wave source (around 30°S, between 150°W and 110°W), where anomalous convective activity is noticed, and descending vertical motion at the equator coinciding with the subsidence branch of the zonal Walker cell described above. The upper level convergence and subsidence in central/eastern equatorial Pacific act together with the above described Hadley cell circulation for inducing a tropical–extratropical teleconnection via a stationary atmospheric Rossby wave. A u-shaped wave-like teleconnection pattern with alternated centres of low and high pressure anomalies is observed towards South America. This wave-like pattern presents a barotropic structure with two co-located anomalous high pressure centres in upper and lower levels of the atmosphere in the vicinities of South America, one over the Pacific and one over the Atlantic, and an anomalous low pressure centre in the southern tip of South America. The anomalous high pressure centre over the South Atlantic acts to block the migration of low pressure (frontal) systems over the southeast region of Brazil and also favours the maintenance of warm sea surface temperatures near the coast of southeast Brazil via direct solar radiation reaching the ocean surface. The associated anomalous anticyclone circulation over the Atlantic extends over the southeast region of Brazil and transports drier than normal air from the Atlantic towards this region, and more humid than normal air from the Amazon toward southern Brazil. This represents a diversion of the traditional humidity flux from the Amazon region towards the southeast region of Brazil performed by the low level jet. Consequently, less SACZ episodes are observed with well below normal precipitation recorded over the southeast region of Brazil, configuring drought conditions with important impacts.

Acknowledgments The research leading to these results has received funding from the SPECS project (Grant Agreement No. 308378) funded by the European Commission's Seventh Framework Research Programme. C.A.S.C. and T.A. were supported by Conselho Nacional de Desenvolvimento Científico e Tecnológico (CNPq) processes 306863/2013-8 and 300976/2010-0, respectively. T.A. also had the support from FAPESP (Proc. No. 2008/58101-9) and Vale Technological Institute. The National Meteorological Service (INMET) and regional meteorological centres in Brazil are acknowledged for making available the observed precipitation data used in this study. We thank Simone T. Ferraz and Ana Carolina V. Freitas for their help with Figs. 8 and 9. Two anonymous reviewers are thanked for providing constrictive criticisms that helped improved the quality of the paper.

References

Bombardi RJ, Carvalho LMV, Jones C, Reboita MS (2013) Precipitation over eastern South America and the South Atlantic Sea surface temperature during neutral ENSO periods. Clim Dyn 42:1553–1568

Brankovic C, Palmer TN, Ferranti L (1994) Predictability of seasonal atmospheric variations. J. Clim 7:217–237

Charney JG, Shukla J (1981) Predictability of monsoons. In: Lighthill J, Pearce R (eds) Monsoon dynamics. Cambridge University Press, Cambridge, pp 99–109

Coelho CAS, Cardoso DHF, Firpo MAF (2015) Precipitation diagnostics of an exceptionally dry event in São Paulo, Brazil. Theor Appl Climatol. doi:10.1007/s00704-015-1540-9

Drumond ARM, Ambrizzi T (2005) The role of SST on the South American atmospheric circulation observed during the 2000/2001 austral summer. Clim Dyn 24:781–791

Espinoza JC, Marengo JA, Ronchail J, Carpio JM, Flores LN, Guyot JL (2014) The extreme 2014 flood in south-western Amazon basin: the role of tropical–subtropical South Atlantic SST gradient. Environ Res Lett. doi:10.1088/1748-9326/9/12/124007

Grimm AM (2003) The El Niño impact on summer monsoon in Brazil: regional processes versus remote influences. J Clim 16:263–280

Grimm AM, Silva Dias PL (1995) Analysis of tropical–extratropical interactions with influence functions of a barotropic model. J Atmos Sci 52:3538–3555

Grimm AM, Zilli MT (2009) Interannual variability and seasonal evolution of summer monsoon rainfall in South America. J Clim 22:2257–2275

Grimm AM, Pal J, Giorgi F (2007) Connection between spring conditions and peak summer monsoon rainfall in South America: role of soil moisture, surface temperature, and topography in eastern Brazil. J Clim 20:5929–5945

Herdies DL, DaSilva A, Silva Dias MAF, Ferreira RN (2002) The moisture budget of the bimodal pattern of the summer circulation over South America. J Geophys Res 107(D20):8075. doi:10.1029/2001JD000997

Hoskins BJ, Ambrizzi T (1993) Rossby wave propagation on a realistic longitudinaly varying flow. J Atmos Sci 50:1661–1671

Kalnay et al (1996) The NCEP/NCAR 40-year reanalysis project. Bull Am Meteorol Soc 77:437–470

Kodama YM (1992) Large-scale common features of sub-tropical precipitation zones (the Baiu Frontal Zone, the SPCZ, and the SACZ). Part I: characteristics of subtropical frontal zones. J Meteorol Soc Jpn 70:813–835

Kodama YM (1993) Large-scale common features of sub-tropical precipitation zones (the Baiu Frontal Zone, the SPCZ, and the SACZ). Part II: conditions of the circulations for generating the STCZs. J Meteorol Soc Jpn 71:581–610

Kousky VE (1979) Frontal influences on northeast Brazil. Mon Weather Rev 107:1142–1153

Marengo JA, Douglas M, Silva Dias P (2002) The South American low-level jet east of the Andes during the LBA-TRMM and WET AMC campaign of January–April 1999. J Geophys Res 107(47):1–11

Nogués-Paegle J, Mo KC (1997) Alternating wet and dry conditions over South America during summer. Mon Weather Rev 125:279–291

Porto RL, Porto MFA, Palermo M (2014) A ressurreição do volume morto do Sistema Cantareira na Quaresma. Rev DAE 62(197):18–25. doi:10.4322/dae.2014.131

Rayner NA, Parker DE, Horton EB, Folland CK, Alexander LV, Rowell DP, Kent EC, Kaplan A (2003) Global analyses of sea surface temperature, sea ice, and night marine air temperature since the late nineteenth century. J Geophys Res 108(D14):4407. doi:10.1029/2002JD002670

Reboita MS, Da Rocha RP, Ambrizzi T, Gouveia CD (2014) Trend and teleconnection patterns in the climatology of extratropical cyclones over the southern hemisphere. Clim Dyn. doi:10.1007/s00382-014-2447-3

Sardeshmukh PD, Hoskins BJ (1988) The generation of global rotational flow by steady idealized tropical divergence. J Atmos Sci 45(7):1228–1251

Schneider U, Becker A, Finger P, Meyer-Christoffer A, Ziese M, Rudolf B (2014) GPCC's new land surface precipitation climatology based on quality-controlled in situ data and its role in quantifying the global water cycle. Theor Appl Climatol 115:15–40. doi:10.1007/s00704-013-0860-x

Yang G-Y, Hoskins BJ (1996) Propagation of Rossby waves of nonzero frequency. J Atmos Sci 53:2365–2378